American Mineralogist, Volume 64, pages 788–798, 1979

The structure of vanadium-bearing tourmaline and its implications regarding tourmaline solid solutions

FRANKLIN F. FOIT, JR. AND PHILIP E. ROSENBERG

Department of Geology, Washington State University
Pullman, Washington 99164

Abstract

The structure of an alkali cation-deficient, vanadium tourmaline has been refined (R = 0.041 for 2727 intensity data) in order to evaluate the effects of tourmaline composition on structural distortion. V-tourmaline, $(Na_{0.44}Ca_{0.36}Mg_{0.18}K_{0.02})(Mg_{1.87}V^{3+}_{0.76}Cr^{3+}_{0.19}Fe^{2+}_{0.18})(Al_{5.56}V^{3+}_{0.38}Ti^{4+}_{0.06})(Si_{5.63}Al_{0.37})(B_{2.98}\square_{0.02})O_{27}(O_{1.10}OH_{2.58}F_{0.32})$, is rhombohedral with a = 15.967(2) and c = 7.191(1)A; space group $R3m$. Despite compositional differences the structure is very similar to those of other members of the tourmaline group, most notably a recently refined aluminous dravite. Analysis of tourmaline-group structural data reveals (1) a negative correlation between tetrahedral bond angle variance and mean "alkali"(3a)–oxygen bond length; (2) negative correlations between both 9b and 18c octahedral angle variances and mean 9b–O bond length; (3) a negative correlation between ditrigonality and 9b octahedral angle variance; (4) a positive correlation between weighted mean octahedral bond length and cell volume; and (5) a positive correlation between Na occupancy in the 3a site and mean 3a–O bond length. These observations demonstrate a systematic flexibility of the structure in response to diverse cation substitution.

The lack of a distinct coupling between the sizes of the 9b and 18c octahedra in refined tourmaline structures and the extensive and possibly complete substitution of Al^{3+} in the 9b site in tourmalines suggest that the presence of cations that can vary in size (*e.g.*, $Fe^{2+,3+}$) in order to create a compatible edge may not be a prerequisite for dravite–elbaite solid solution. In view of the structural flexibility of tourmaline and the ease of proton exchange to maintain charge balance, the apparent immiscibility of dravite and elbaite is thought to reflect extreme fractionation of Mg and Li during petrogenesis and by the tourmaline structure, due to the large difference in the field strengths of these cations. Other major features of tourmaline substitutional chemistry are also rationalized on the basis of cation field strength.

Introduction

The crystal chemistry of the tourmaline group is exceedingly complex. In addition to solid-solution series extending from schorl to dravite and from schorl to elbaite, Foit and Rosenberg (1974, 1975, 1977) reported the existence of two additional substitutions (1) $R^+ + R^{2+} = R^{3+} + \square$ and (2) $H^+ + R^{2+} = R^{3+}$ in natural tourmalines of the schorl–dravite series, which together result in solid solution toward an alkali cation–deficient series, $R^+_{1-x}R^{3+}_3R^{3+}_6(BO_3)_3Si_6O_{18}O_{3-x}(OH)_{1+x}$.

The extent of substitution in any structure is determined not only by the coordination and dimensions of the sites available for substitution and the tolerance of the structure to distortion, but also by the characteristics of the ions themselves (*e.g.*, field strength). While a large amount of structural data on members of the tourmaline group (dravite, Buerger *et al.*, 1962; buergerite, Barton, 1969; elbaite, Donnay and Barton, 1972; schorl, Fortier and Donnay, 1975; uvite and an aluminous dravite, Schmetzer, 1978) has accumulated over the past 15 years, systematic structural changes produced by these substitutions have not been deciphered. The structure of a significantly alkali cation-deficient, vanadium-rich tourmaline has been examined and analyzed in conjunction with all available tourmaline structural data in an attempt to evaluate the structural significance of cation substitution. It was anticipated that this study would lead to a better understanding of the role of structural distortion and cation field strength (Weyl and Marboe, 1962) in limiting tourmaline composition.

0003–004X/79/0708–0788$02.00

Vanadium-bearing tourmaline

Specimen description and chemistry

Snetsinger (1966) reported the occurrence of an unusually vanadium-rich tourmaline coexisting with quartz, graphite, barium–vanadium muscovite, and biotite in a quartz graphite schist at Silver Knob, Mariposa County, California. The crystals were found to be compositionally zoned with cores appreciably deficient in alkali (alkaline earth) cations.

A large number of tourmaline fragments were separated, using heavy liquids, from a ground hand specimen of schist from this locality. Although crystals suitable for X-ray analysis were difficult to isolate due to the abundance and fine dispersal of graphite throughout the rock, an equant (~0.3 mm in diameter), optically uniform fragment of the core zone was finally extracted from the tourmaline fraction.

An electron microprobe analysis of this crystal is given in Table 1. Analyses made at many points on the crystal showed it to be essentially homogeneous. Only one element, V, showed a statistically significant variation, and this corresponded to a decrease of less than 0.25 weight percent at one edge of the crystal. Vanadium and the small amount of iron present were initially assumed to be in the 3+ and 2+ valence states, respectively. Water was obtained by difference. Since increasing the valence states of iron and/or vanadium reduces the apparent amount of water, the amount indicated in Table 1 represents a maximum value for this crystal. A comparison of calculated and ideal anionic valence sums for the vanadium tourmaline structure (see Discussion) suggests that the actual proton content may be slightly lower.

Despite the deficiency of alkali cations, the alkali site (3a) appears to be fully occupied. An excess of cations (Mg^{2+}, Fe^{2+}, Cr^{3+}, V^{3+}, Ti^{4+}) normally found in octahedral coordination which is equal to the alkali cation deficiency strongly suggests that Mg^{2+} (or, less likely, Fe^{2+}) partially occupies the alkali site (Table 1).

Table 1. Vanadium tourmaline. Microprobe analysis

Oxide	Wt. percent*	Numbers of ions
SiO_2	33.61	5.63
B_2O_3	10.3	2.98
Al_2O_3	30.03	5.93
Cr_2O_3	1.48	0.19
V_2O_3	8.52	1.14
MgO	8.23	2.05
TiO_2	0.45	0.06
FeO	1.25	0.18
MnO	0.00	0.00
Na_2O	1.34	0.44
CaO	2.02	0.36
K_2O	0.11	0.02
	97.94	
Less O = F	-0.25	$\rho_{calc} = 3.165$
	97.69	
H_2O	2.31	
	100.00	

Formula on the basis of 31(O,OH,F): $(Na_{0.44}Ca_{0.36}Mg_{0.18}K_{0.02})(Mg_{1.87}V^{3+}_{0.76}Cr^{3+}_{0.19}Fe^{2+}_{0.18})(Al_{5.56}V^{3+}_{0.38}Ti^{4+}_{0.06})(Si_{5.63}Al_{0.37})B_{2.98}\square_{0.02}O_{27}O_{1.10}(OH_{2.58}F_{0.32})$

* An average of analyses at 5 different locations on the crystal.

Unit cell and intensity data collection

X-ray photographs displayed diffraction symmetry and lattice extinctions compatible with space group *R*3*m*. All reflections were sharp; no weak or diffuse "extra" reflections were observed on long-exposure photographs. The unit-cell parameters, $a = 15.967$ (2) and $c = 7.191(1)$A, were obtained by least-squares refinement of 12 high-angle reflections collected using a computer controlled Picker 4-circle diffractometer and Mo$K\alpha$ radiation.

A total of 2727 reflection intensities was collected using a 0.05° step scan size, a 2-second step count, and a 20-second background count. While 1645 reflections were collected in the 60° $a_1^* a_2^* c^*$ wedge over a range $2\theta = 5$–90°, only 1082 were collected in the $-a_1^*-a_2^*-c^*$ wedge, due to a diffractometer arrangement limiting the accessible 2θ region to 5–75°. Three standard reflections representing a wide range of intensity were measured after every 50 reflections in order to monitor long-term diffractometer performance. The data were corrected for Lorentz and polarization effects, but absorption effects were neglected because of the approximate spherical shape of the crystal and its low linear absorption coefficient ($\mu = 16.8$ cm^{-1}). Subsequent refinement was carried out using the 2602 structure factors for which $F_{obs} > 3\sigma(F_{obs})$.

Refinement

Least-squares refinement was undertaken using a modified versions of ORFLS written by Busing *et al.*

Table 3. Vanadium tourmaline. Atom positional and thermal parameters (standard deviations in parentheses)

Atom	Position	x	y	z	B*	β_{11}**	β_{22}	β_{33}	β_{12}	β_{13}	β_{23}
Na,Ca,Mg	3a	0	0	0.21764(21)	1.50(3)	196(3)	β_{11}	670(20)	$\beta_{11}/2$	0	0
Mg,V,Cr,Fe	9b	0.12353(3)	x/2	0.63364(8)	0.446(9)	58(2)	42(1)	306(6)	$\beta_{11}/2$	-47(3)	$\beta_{13}/2$
Al,V,Ti	18c	0.29782(3)	0.26152(3)	0.61011(8)	0.353(7)	44(1)	51(1)	181(5)	22(1)	1(2)	11(2)
B	9b	0.10976(7)	2x	0.45178(30)	0.40(3)	46(5)	41(7)	277(26)	$\beta_{22}/2$	$\beta_{23}/2$	-2(2)
Si,Al	18c	0.19173(2)	0.18990(3)	0	0.333(6)	39(1)	39(1)	192(5)	18(1)	-2(2)	-9(2)
O(1)	3a	0	0	0.77026(39)	0.72(4)	113(6)	β_{11}	341(38)	$\beta_{11}/2$	0	0
O(2)	9b	0.06085(5)	2x	0.48140(24)	0.79(3)	99(4)	48(5)	541(24)	$\beta_{22}/2$	$\beta_{23}/2$	22(9)
O(3)	9b	0.26387(13)	x/2	0.50919(23)	0.78(2)	187(7)	104(4)	242(19)	$\beta_{11}/2$	11(10)	$\beta_{13}/2$
O(4)	9b	0.09306(6)	2x	0.07162(23)	0.76(3)	75(4)	157(7)	398(22)	$\beta_{22}/2$	$\beta_{23}/2$	-28(10)
O(5)	9b	0.18444(13)	x/2	0.09256(22)	0.78(3)	180(7)	71(3)	420(22)	$\beta_{11}/2$	4(10)	$\beta_{13}/2$
O(6)	18c	0.19548(7)	0.18576(7)	0.77616(15)	0.54(2)	87(4)	82(4)	218(12)	44(3)	-8(6)	-21(6)
O(7)	18c	0.28559(7)	0.28536(7)	0.07803(15)	0.61(2)	73(4)	63(3)	294(14)	14(3)	-30(6)	-15(6)
O(8)	18c	0.20903(7)	0.26984(7)	0.43879(17)	0.60(2)	36(3)	80(4)	484(15)	27(3)	19(6)	40(6)
H[O(3)]	9b	0.2615(27)	x/2	0.3901(57)	-0.17(57)						

* Isotropic temperature factors are from the last cycle of refinement before changing to anisotropic temperature factors.

** x 10^5

(1962). Initial position parameters were those of buergerite (Barton, 1969). The form factor tables were formulated from the data of Cromer and Waber (1965) for neutral atoms and the anomalous dispersion coefficients given in *International Tables for X-ray Crystallography*. The observed structure factors (F_o) were weighted on the basis of $1/\sigma_F^2$, where σ_F is the standard deviation of F_o based on counting statistics.

The weighted residual (R_w) converged to a value of 0.060 after several cycles of refinement during which the scale factor, atom coordinates, and isotropic temperature factors were varied. Comparison of ratio $F_o(511)/F_o(\bar{5}11)$ to that observed for buergerite, from which the absolute orientation of the structure had been determined (Barton, 1969), indicated that the indexing of the vanadium tourmaline data set needed to be transformed ($hkl \rightarrow kh\bar{l}$) to be compatible with the conventional orientation. Subsequent refinement using the transformed data set reduced R_w to 0.042 and resulted in reasonable isotropic temperature factors for all atoms.

The cation occupancy of the 18c and 9b octahedral sites was determined by monitoring the residual and temperature factors as the relative proportions of "light" (L = 0.60Al + 0.40Mg) and "heavy" (Hv = 0.69V + 0.16Cr + 0.13Fe + 0.02Ti) atoms were varied. Minima in the residuals (R = 0.041 and R_w = 0.047) and isotropic temperature factors of 0.35 and 0.45 for the 18c and 9b "atoms," respectively (Table 3), were achieved with distributions corresponding to 18c = $L_{0.92}Hv_{0.08}$ and 9b = $L_{0.63}Hv_{0.37}$.

Several cycles of least squares, during which position and anisotropic thermal parameters and scale factor were varied, further reduced the residuals R and R_w to 0.029 and 0.035, respectively. Refinement of the proton positions was then undertaken, using the positional parameters determined from neutron diffraction studies of buergerite (Tippe and Hamilton, 1971). However, only the positional and isotropic thermal parameters of the hydrogen atom bonded to O(3) could be varied successfully. This is due, no doubt, to its higher multiplicity compared to the hydrogen atom presumed to be bonded to the O(1) oxygen atom. The refinement was completed by simultaneously varying all positional and anisotropic thermal parameters (except for hydrogen, which was varied isotropically). The final residuals are R = 0.028, R_w = 0.034 for the 2602 data used in the refinement and R = 0.033, R_w = 0.041 for the 2727 data collected (Table 2[1]). The positional and thermal parameters are listed in Table 3. The dimensions and

orientations of the thermal ellipsoids (Table 4[1]) and the interatomic distances and angles (Table 5, uncorrected for thermal motion) were calculated using the Fortran function and error program ORFFE (Busing *et al.*, 1964).

Discussion

Vanadium tourmaline structure and its relationship to other refined tourmaline structures

The structure of vanadium tourmaline is very similar to those of other refined tourmaline structures (dravite, Buerger *et al.*, 1962; buergerite, Barton, 1969; elbaite, Donnay and Barton, 1972; schorl, Fortier and Donnay, 1975; uvite and aluminous dravite, Schmetzer, 1978), most notably aluminous dravite. For this reason, only the details of the structure and structural comparisons will be given. The reader is referred to two excellent diagrams (Buerger *et al.*, 1962; Barton, 1969) which portray the general configuration of the structure.

Tetrahedral ring. The mean T–O bond length (1.625A) in vanadium tourmaline is the largest yet observed for a tourmaline structure. This is to be expected, since Al^{3+}-for-Si^{4+} substitution ($Si_{5.63}Al_{0.37}$) is greater in vanadium tourmaline than in any other natural tourmaline structure refined to date. The only other tourmaline with a significant amount of Al^{3+}-for-Si^{4+} substitution, dravite (Buerger *et al.*, 1962), has the second largest mean T–O bond length (1.621A).

Variances in the O–T–O angles $\sigma^2_{\theta(\text{tet})}$, which have been used as a measure of distortion (Robinson *et al.*, 1971), are apparently related to the mean "alkali cation" (3a-site cation)–oxygen bond length; they gradually decrease with increasing mean "alkali"–oxygen bond length (Fig. 1). This is consistent with the fact that each 3a coordination polyhedron shares the six contiguous interior basal edges of the ring. Thus, any variation in the size of the cation in the 3a site should affect the configuration of the ring and/or its individual tetrahedra. A similar coupling of tetrahedral distortion to effective {X} cation size (Ca^{2+}, Mg^{2+}, Fe^{2+}, Mn^{2+}) was observed in the garnets (Robinson *et al.*, 1971). While use of angular variance for dravite might be questioned on the grounds that dravite may have been refined in the wrong absolute orientation (Barton, 1969), refinement of vanadium tourmaline in both orientations yielded variances and mean bond lengths which differed by insignificant amounts.

Ditrigonality, δ, defined by Barton (1969) as a measure of the distortion of the T_6O_{18} ring from hexagonal symmetry, is 0.009 for vanadium tourmaline. This is closer to the values for elbaite (0.009) and schorl (0.005) than to aluminous dravite (0.019), uvite (0.029), dravite (0.032), and buergerite (0.038). The only structural parameter which appears to be correlated to ditrigonality is 9b octahedral angle variance (Fig. 2). This apparent negative correlation is not unexpected, because of vertex sharing between the 9b octahedra and the Si tetrahedra of the ring. The reason for the gross deviation of buergerite from the general trend remains obscure.

Table 5. Vanadium tourmaline. Interatomic distances and angles (standard deviations in parentheses)

Atoms		Distance (Å)	Atoms		Distance (Å)	Angles (°)
Si-O(4)		1.630(1)	O(4) - O(5)		2.567(2)	103.19(7)
Si-O(5)		1.646(1)	O(4) - O(7)		2.663(1)	110.31(7)
Si-O(6)		1.613(1)	O(5) - O(7)		2.674(1)	110.45(6)
Si-O(7)		1.612(1)	O(6) - O(4)*		2.683(2)	111.64(7)
			O(6) - O(5)*		2.679(2)	110.56(7)
Mean		1.625	O(6) - O(7)		2.650(1)	110.49(5)
			Mean		2.653	
B-O(2)		1.369(1)	$O(8)^1$- O(2)	2x	2.385(1)	120.7(1)
$B\text{-}O(8)^1$	2x	1.376(1)	O(8) - $O(8)^1$		2.367(3)	118.6(1)
Mean		1.374	Mean		2.379	
Mg-O(1)		1.971(2)	O(1) - $O(2)^2$	2x	2.673(3)	84.15(6)
$Mg\text{-}O(2)^2$	2x	2.018(1)	O(1) - $O(6)^3$	2x	3.047(1)	100.10(6)
Mg-O(3)		2.137(2)	O(2) - $O(2)^2$		2.915(1)	92.45(6)
$Mg\text{-}O(6)^3$		2.004(1)	$O(2)^7$- $O(6)^3$	2x	2.822(2)	89.09(5)
			O(3) - $O(2)^2$	2x	3.169(2)	99.37(6)
Mean		2.026	O(3) - $O(6)^3$	2x	2.560(2)	76.31(4)
			O(6) - $O(6)^3$		2.811(3)	89.07(8)
			Mean		2.856	
Al-O(3)		1.995(1)	O(3) - O(6)		2.560(2)	82.33(6)
Al-O(6)		1.893(1)	O(3) - $O(7)^5$		2.888(2)	95.67(6)
$Al\text{-}O(7)^4$		1.955(1)	O(3) - O(8)		2.793(2)	90.64(6)
$Al\text{-}O(7)^5$		1.900(1)	O(3) - $O(8)^5$		2.891(2)	95.80(7)
Al-O(8)		1.932(1)	O(6) - O(8)		2.729(2)	91.00(5)
$Al\text{-}O(8)^5$		1.900(1)	O(6) - $O(8)^5$		2.793(2)	94.86(6)
			$O(7)^4$- O(6)		2.784(2)	92.69(6)
Mean		1.929	$O(7)^4$- $O(7)^5$		2.738(1)	90.50(2)
			$O(7)^4$- O(8)		2.898(2)	77.64(6)
			$O(7)^5$- O(8)		2.417(1)	96.41(6)
			$O(7)^5$- $O(8)^5$		2.825(2)	78.20(5)
			$O(7)^4$- $O(8)^5$		2.417(1)	96.08(5)
			Mean		2.728	
$Na\text{-}O(2)^{2,6}$	3x	2.536(2)	$O(2)^2$- $O(2)^{2,6}$	3x	2.9149(3)	70.17(6)
$Na\text{-}O(4)^{2,6}$	3x	2.780(1)	$O(2)^{2,6}$-$O(4)^{2,6}$	3x	3.0784(23)	70.61(4)
$Na\text{-}O(5)^{2,6}$	3x	2.704(2)	$O(2)^{2,6}$-$O(5)^{2,6}$	6x	3.5865(23)	86.32(4)
			$O(4)^2$- $O(4)^{2,6}$	3x	4.4576(6)	106.61(5)
Mean		2.673	$O(4)^{2,6}$-$O(5)^{2,6}$	6x	2.5665(9)	55.79(4)
			Mean		3.251	
H-O(3)		0.86(4)	O(3) - O(5)		3.191(2)	154.(2)
H-O(5)		2.39(4)				

1 = y-x,y,z; 2 = y-x,-x,z; 3 = x,x-y,z; 4 = y-x+1/3,-x+2/3,z+2/3; 5 = -y+2/3,x-y+1/3,z+1/3; 6 = -y,x-y,z transformations relating coordinates to those of Table 4.

* = positioned in an adjacent unit cell.

[1] To obtain a copy of Tables 2 and 4, order Document AM-79-106 from the Business Office, Mineralogical Society of America, 2000 Florida Ave., NW, Washington, DC 20009. Please remit $1.00 in advance for the microfiche.

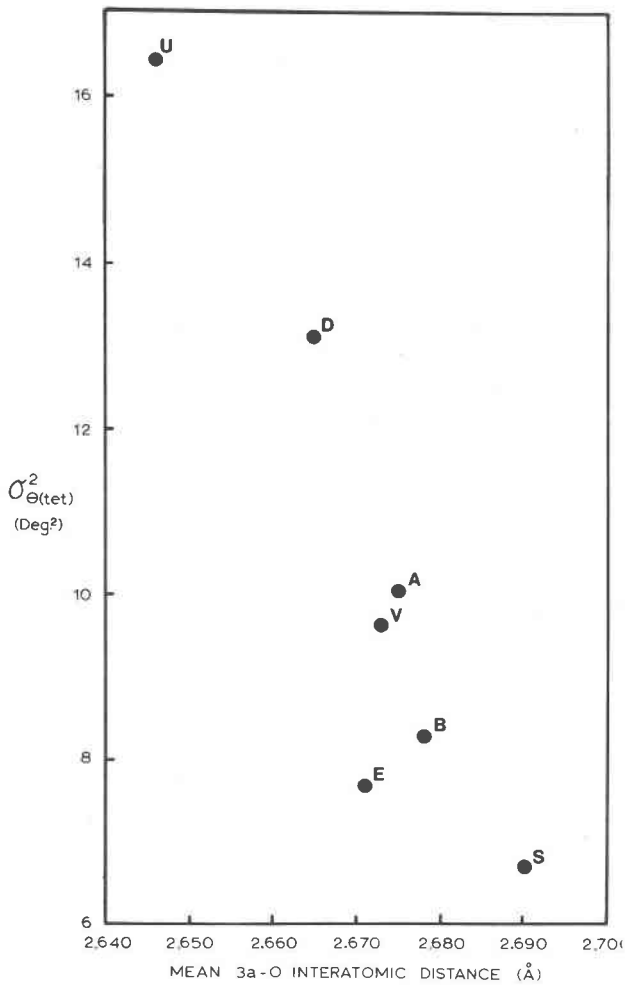

Fig. 1. Variation of tetrahedral bond angle variance, $\sigma^2_{\theta(tet)}$, with mean 3a–O interatomic distance (A = aluminous dravite, B = buergerite, D = dravite, E = elbaite, S = schorl, U = uvite, V = vanadium tourmaline).

Octahedral portion. In vanadium tourmaline there is a significantly greater scattering power associated with the larger more distorted 9b site ($L_{0.63}Hv_{0.37}$) than with the smaller less distorted 18c site ($L_{0.92}Hv_{0.08}$). This is in keeping with the results of other transition-metal tourmaline refinements (buergerite, Barton, 1969; schorl, Fortier and Donnay, 1975). A comparison of the mean 18c–O bond length and site occupancy (1.926A, $L_{0.92}Hv_{0.08}$) of vanadium tourmaline to those of elbaite (1.905A, $Al_{1.00}$) and schorl (1.922A, $Al_{0.93}Fe^{2+}_{0.07}$) is in accord with very little substitution of cations other than Al in this site. Thus, the formula $(Na_{0.44}Ca_{0.36}Mg_{0.18}K_{0.02})(Mg_{1.87}Hv_{1.87}Hv_{1.13})(Al_{5.56}\ Hv_{0.44})(Si_{5.63}Al_{0.37})B_{2.98}O_{27}O_{1.10}(OH_{2.58}F_{0.32})$, which is very similar to the one proposed on the basis of the analytical data (Table 1), adequately describes the site chemistry of vanadium tourmaline.

While very little substitution of cations other than Al has been observed in the smaller 18c site (Tsang *et al.*, 1971), the larger more distorted 9b site with which it shares an edge tolerates extensive as well as diverse substitutions, producing a substantial variation in mean bond length. The angular variance (distortion) of both the 9b and 18c octahedra in tourmaline appears to be negatively correlated to mean 9b–O bond length, smaller size producing greater distortion (Figs. 3, 4). However, no distinct correlation between the size of the 18c site and its angular variance was observed. The predominant influence of the mean 9b–O bond length over the 18c–O bond length in controlling 18c octahedral distortion is thought to reflect the significantly greater variability in the size of the 9b site. The larger angular variance in schorl (Fig. 3) than might be expected on the basis of 9b site size may be due, in part, to the Jahn-Teller effect (Walsh *et al.*, 1974).

The volume of the unit cell varies non-linearly with the dimensions of the 9b and 18c octahedra (Fig. 5); the greater the mean 9b–O and 18c–O bond lengths, the greater the cell volume. This accounts for the success of the often-used Epprecht (1953)-type diagram, by which cell parameters have been shown to vary as a function of substitution between schorl–dravite and schorl–elbaite. The relationships between

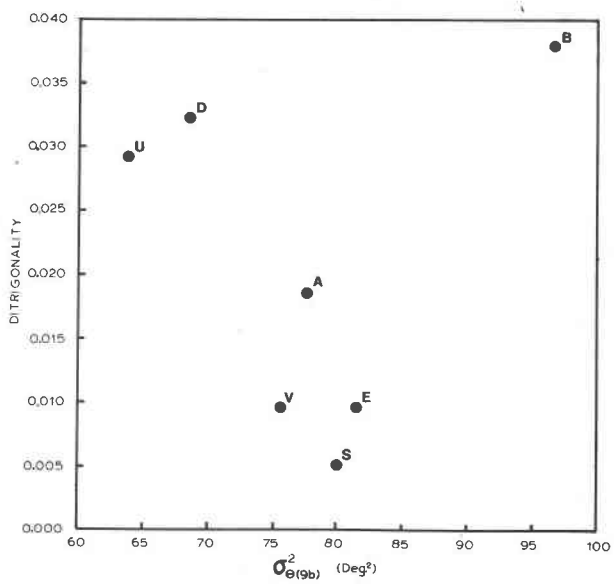

Fig. 2. Variation of ditrigonality, δ, (δ = $(r_l - r_s)/r_s$ where r_l and r_s are the distances from the three-fold axis to O(4) and O(5), respectively) with 9b octahedral angle variance, $\sigma^2_{\theta(9b)}$.

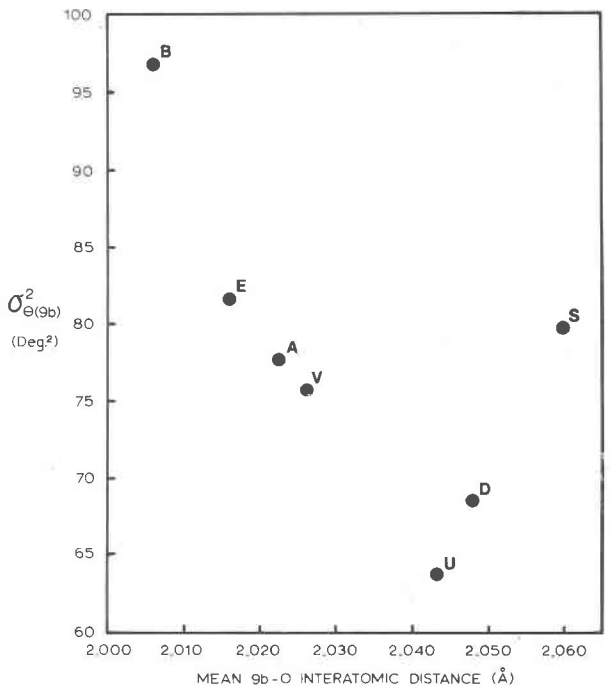

Fig. 3. Variation of 9b octahedral angle variance, $\sigma^2_{\theta(9b)}$, with mean 9b–O interatomic distance.

tourmaline cell volume and mean octahedral bond lengths and between mean 9b–O bond length and 18c octahedral distortion is not surprising, in view of the fact that edge-sharing between the 9b and 18c octahedra results in a quasi-rigid three-dimensional octahedral framework.

Alkali cation site. The 3a site appears to be constrained by the octahedral (9b) and tetrahedral portions of the structure, and therefore is only capable of adjusting its size within restricted limits to variations in cation occupancy. A plot of Na (largest abundant alkali cation in tourmaline) content *vs.* mean alkali–oxygen bond length (Fig. 6) reveals a positive correlation between sodium content and the size of the 3a coordination polyhedron. However, if mean 3a site–oxygen interatomic distance is plotted against either the effective radius of the cations occupying that site or cell volume (Fig. 5), no correlation can be observed, indicating that the octahedral and tetrahedral portions of the structure tend to hold the site open when cations smaller than Na occupy the site. This conclusion is in accord with the absence of a correlation between cell volume and 3a site occupancy observed in a study of tourmalines synthesized in the system $MgO–Al_2O_3–SiO_2–B_2O_3–H_2O$ (Rosenberg and Foit, 1977), and demonstrates the relative insignificance of alkali-site occupancy as compared to octahedral-site occupancy in determining cell parameters.

Protons. The principal hydrogen bonds involve two non-equivalent oxygen atoms, O(1) with the bond direction paralleling the 3-fold axis and O(3) with the bond lying in the mirror plane. While it was possible to refine the positional parameters of one of the protons successfully, revealing a hydrogen bond geometry, H–O(3) = 0.86(4)A, H–O(5) = 2.39(4)A and O(3)–H ··· O(5) = 154(2)°, comparable to that reported for buergerite (Tippe and Hamilton, 1971), no information regarding the partial occupancy of either the O(1) or the O(3) proton site could be obtained from the X-ray results. An indirect estimation of proton occupancy was obtained, using the method of Donnay and Allmann (1970) (Table 6). Although the discrepancy value Δrms = 0.054, a measure of the agreement between calculated and ideal valence sums is comparable to those reported for other tourmalines (Fortier and Donnay, 1975), the charge imbalance for O(1) and O(3) is unusually large. This suggests that vanadium tourmaline has a slightly lower proton content than indicated by the analytical data, and that some of the V and/or Fe is in a higher valence state. The oxidation state and site distribution of vanadium in tourmaline from this locality is currently being studied using optical absorption techniques by G. Rossman (personal communication).

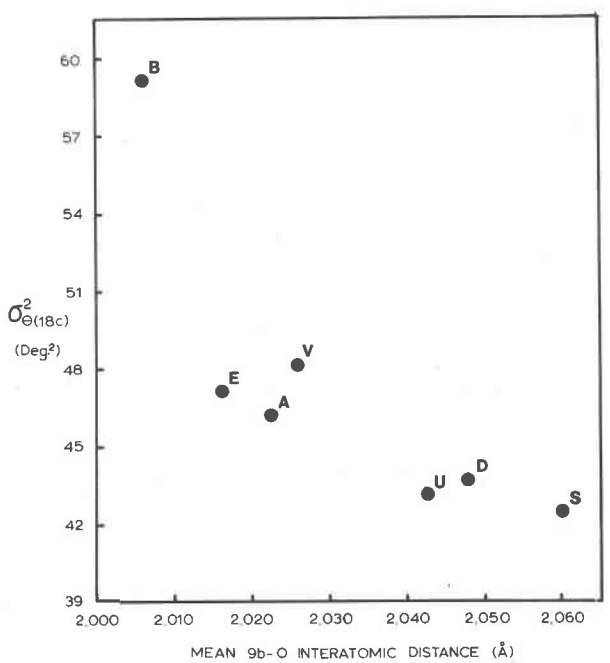

Fig. 4. Variation of 18c octahedral angle variance, $\sigma^2_{\theta(18c)}$, with mean 9b–O interatomic distance.

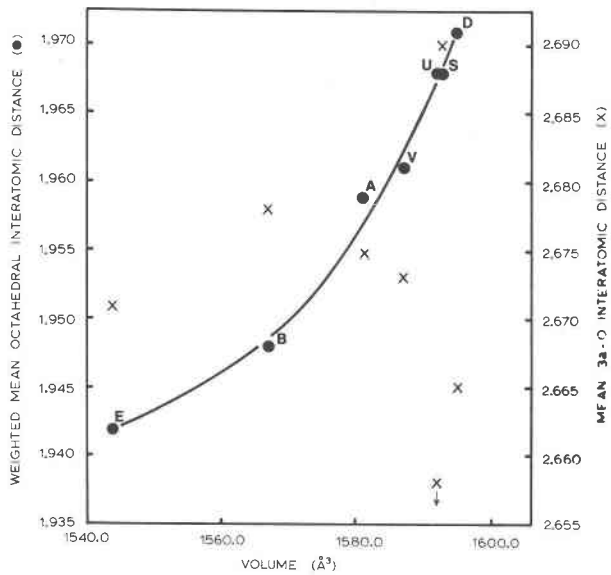

Fig. 5. Variation of cell volume with weighted mean octahedral, $[\overline{9b\text{–}O} + 2(\overline{18c\text{–}O})]/3$, and with mean 3a–O interatomic distance. The mean 3a–O distance in uvite is 2.646A and lies below the abscissa.

Solid solution relationships: structural considerations

As observed in previous investigations (Buerger *et al.*, 1962; Barton, 1969; Donnay and Barton, 1972; Fortier and Donnay, 1975) the tourmaline structure seems to be remarkably tolerant of diverse substitutions. Despite extensive dehydroxylation relative to schorl, elbaite, and dravite according to the substitution $H^+ + R^{2+}_{(9b)} = R^{3+}_{(9b)}$, as well as substitution of Mg^{2+} into the 9-coordinated 3a-"alkali" site (Foit and Rosenberg, 1977; Rosenberg and Foit, 1977), the structural configuration of vanadium tourmaline appears to be intermediate between these end-members (Figs. 1–5).

Studies of both natural aluminous dravites (Table 7, Foit and Rosenberg, 1977) and synthetic tourmalines in the system $MgO–Al_2O_3–SiO_2–B_2O_3–H_2O$ (Rosenberg and Foit, 1975, 1977) suggest substantial Al^{3+}-for-Mg^{2+} substitution in the 9b octahedral site (Fig. 7), charge balance being maintained by dehydroxylation, creation of alkali site defects, and/or Al^{3+}-for-Si^{4+} substitution. Similar extensive substitutional relationships involving Al^{3+} and Li^+ in the 9b sites occur in natural elbaites (Table 7, Fig. 7). Synthesis of tourmaline in the system $Na_2O–Al_2O_3–SiO_2–B_2O_3–H_2O$ (Ekambaram, personal communication) demonstrates that the octahedral sites may contain only Al. Thus, extensive and possibly complete substitution of cations (Al^{3+} for Mg^{2+} and Li^+), which represent greatly different sizes ($^{VI}Li = 0.76$, $^{VI}Mg = 0.72$, $^{VI}Al = 0.54$A; Shannon, 1976) and distortions (Figs. 2–4), takes place in the dravites and elbaites.

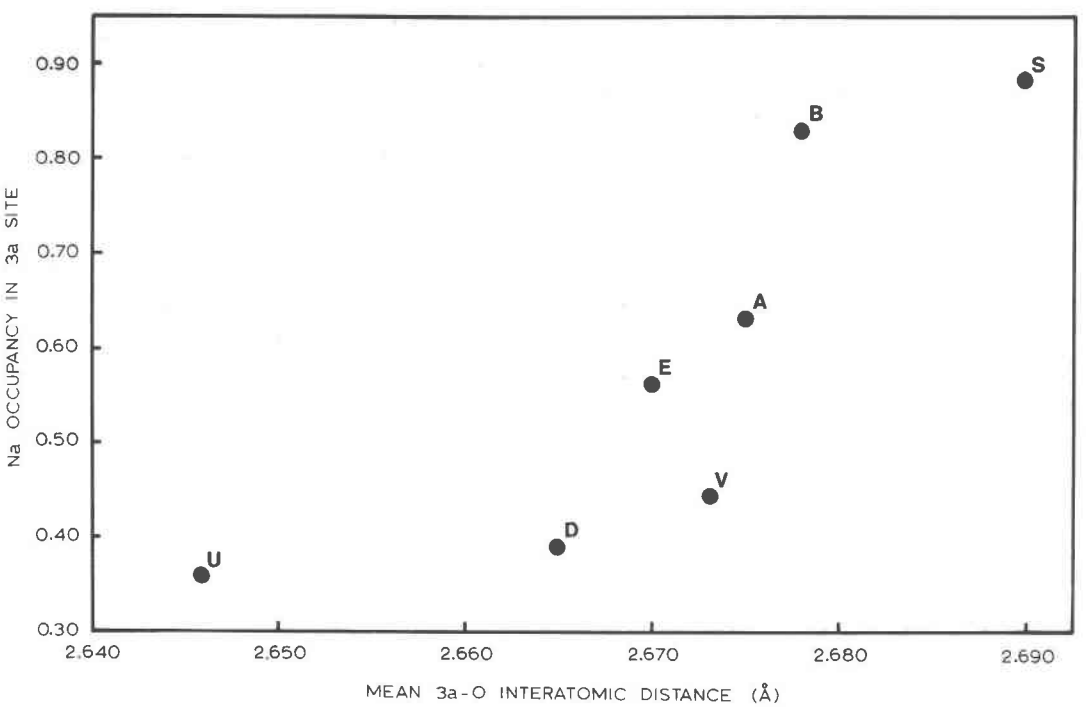

Fig. 6. Variation of mean 3a–O interatomic distance with Na^+ occupancy in the 3a ("alkali") site.

Table 6. Vanadium tourmaline. Bond valences (number of bonds received by anion in parentheses)

Anion	Multi	X 3a	Y 9b	Z 18c	B	Si	$\Sigma_c{}^v$	Anion occupancy	$\lvert\Delta v\rvert$
O(1)	3		0.433 (3)				1.299	$O^{2-}_{0.41}F^-_{0.32}(OH)^-_{0.27}$	0.111
O(2)	9	0.233 (1)	0.402 (2)		1.000 (1)		2.037	O^{2-}	0.037
O(3)	9		0.329 (1)	0.404 (2)			1.137	$(OH)^-_{0.77}O^{2-}_{0.23}$	0.093
O(4)	9	0.131 (1)				0.980 (2)	2.091	O^{2-}	0.091
O(5)	9	0.159 (1)				0.949 (2)	2.057	O^{2-}	0.057
O(6)	18		0.411 (1)	0.559 (1)		1.014 (1)	1.984	O^{2-}	0.016
O(7)	18			0.464 (1) 0.547 (1)		1.016 (1)	2.027	O^{2-}	0.027
O(8)	18			0.547 (1) 0.498 (1)	0.989 (1)		2.034	O^{2-}	0.034
								Δv_{rms} =	0.054
L(Mean)		2.673	2.026	1.929	1.374	1.625			
L(Max)		3.127	2.670	2.268	1.857	2.138			
p(Exp)		5.888	3.145	5.690	2.845	3.168			
V(I)		1.54/9	2.38/6	3.01/6	2.98/3	3.96/4			

Structural configurations required by the nature and extent of coupled substitutions in natural as well as synthetic tourmalines appear to be easily attained, and are not markedly different from those previously reported.

The foregoing data have interesting implications relative to the apparent lack of extensive substitution between dravite and elbaite. The tourmaline structure contains two groups of crystallographically-distinct octahedra; the edge-sharing 18c octahedra which spiral up the 3_1 screw axis and the edge-sharing 9b octahedra which cluster around the 3-fold axis. These octahedra in turn share a common edge O(3)–O(6), forming a three-dimensional octahedral framework. Donnay and Barton (1972) have suggested that, due to the absence of variable valence–variable size cations (*i.e.*, $Fe^{2+,3+}$) along the dravite–elbaite join, the 9b and 18c octahedra cannot achieve configurations permitting a mutual sharing of edges, thereby making the formation of the tourmaline structure impossible. However, no distinct coupling between the sizes of the 9b and 18c octahedra (Fig. 8) is observed in refined tourmaline structures. Furthermore, schorl and elbaite reflect a greater range of 9b–O bond length and 18c octahedral angle variance than do dravite and elbaite (Fig. 4). Yet natural Li-rich tourmalines containing appreciable amounts of Fe^{2+} have been reported, whereas those containing an appreciable amount of Mg^{2+} are unknown, even though these tourmalines may contain multiple-valent cations. If the availability of variable valence cations were an overriding factor limiting the formation of the tourmaline structure, despite possible extensive disordering of cations between the 9b and 18c sites, then natural and synthetic aluminous dravites and natural aluminous elbaites would not form. Thus, there appears to be no obvious structural reason why dravite–elbaite solid solution should not be more extensive than has been observed in natural samples.

Solid solution relationships: field strength considerations

Because of the flexibility of the tourmaline structure and its tolerance of substitutions in several sites, as well as the ease with which protons can be gained

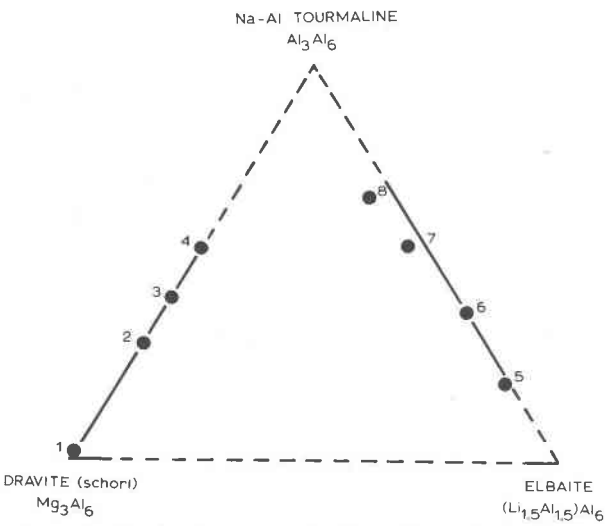

Fig. 7. Extent (solid line) of octahedral substitution between dravite, elbaite and Na–Al tourmaline in natural samples. Numbers refer to samples listed in Table 7. Mg, Li, Al plus minor Fe were considered in plotting tourmaline compositions. Minor amounts of other elements were neglected.

or lost to maintain charge balance, the 9b octahedral site will preferentially be occupied by cations with the highest field strength (Z/a^2, where a = cation–anion interatomic distance; Weyl and Marboe, 1962).

The apparent absence of intermediates between elbaite and dravite in nature (Foit and Rosenberg, 1977) may be due to the extreme fractionation of Mg and Li, both during petrogenesis and by the tourmaline structure as a result of the large difference in the field strength of these cations. Less extreme fractionation between Fe^{2+} and Li^+ due to the somewhat smaller difference in field strengths would account for the greater abundance of elbaite–schorl solid solutions than elbaite–dravite solid solutions in nature (Foit and Rosenberg, 1977).

In the Brown Derby pegmatites, Gunnison County, Colorado, which are believed to have crystallized as a closed system from the walls inward, the atomic proportions of Mg^{2+}, Fe^{2+}, and Mn^{2+} (Staatz *et al.*, 1955) peak and diminish in turn during the crystallization sequence, the first tourmalines being relatively Mg^{2+}- and Fe^{2+}-rich and the last being Li^+-rich (Fig. 9). These data suggest that the highest field strength cations available were preferentially incorporated in the tourmaline structure. The crystallization of tourmaline (and perhaps other minerals) resulted in the depletion of high field strength cations, allowing Li^+ to enter the structure in progressively greater proportions during the later stages of crystallization. If cation field strength typically controls the composition of tourmaline to the same extent as in the Brown Derby pegmatites, then solid solutions between dravite and elbaite would be expected to be very rare in nature.

Field strength can also be used to rationalize the

Table 7. Natural tourmalines for which there appears to be significant Al^{3+}-for-Mg^{2+} and -Li^+ substitution in the 9b octahedral site (calculations based on 31 anions)

1.	$(Na_{0.97}Ca_{0.09}K_{0.02})(Mg_{2.78}Fe_{0.12}Ti_{0.05}Al_{0.03}Li_{0.01}\square_{0.01})Al_6B_{2.99}(Si_{5.96}Al_{0.04})O_{27}O_{0.64}(OH_{3.31}F_{0.05})$
2.	$(Na_{0.57}\square_{0.31}Li_{0.11}Mg_{0.01})(Mg_{2.08}Al_{0.87}Fe_{0.03}Ti_{0.02})Al_6B_{2.82}Si_{6.04}O_{27}O_{0.26}(OH_{3.74}F_{0.03})$
3.	$(\square_{0.67}Na_{0.29}Ca_{0.04})(Mg_{1.66}Al_{1.16}Fe^{3+}_{0.08}Fe^{2+}_{0.07}\square_{0.03})Al_6B_{2.65}Si_{6.25}O_{27}O_{0.64}(OH_{3.46})$
4.	$(Mg_{0.47}Na_{0.41}K_{0.07}\square_{0.05})(Al_{1.52}Mg_{1.35}Ti_{0.11}Fe^{3+}_{0.02})Al_6B_{3.13}Si_{6.30}O_{27}O_{3.84}(OH_{0.16})$
5.	$(Na_{0.71}\square_{0.21}Ca_{0.07}K_{0.01})(Al_{1.61}Li_{1.27}\square_{0.05}Mg_{0.03}Fe^{3+}_{0.03}Mn_{0.01})Al_6B_{3.06}(Si_{5.65}Al_{0.35})O_{26.98}(OH_{3.55}F_{0.47})$
6.	$(Na_{0.56}\square_{0.35}Ca_{0.08}K_{0.01})(Al_{1.74}Li_{1.08}\square_{0.07}Mn_{0.06})Al_6B_{3.04}(Si_{5.95}Al_{0.05})O_{27}O_{0.25}(OH_{3.20}F_{0.55})$
7.	$(Na_{0.69}\square_{0.14}Ca_{0.12}K_{0.05})(Al_{1.93}Li_{0.84}Mg_{0.12}\square_{0.06}Fe^{2+}_{0.03}Fe^{3+}_{0.01}Ti_{0.01})Al_6B_{2.84}(Si_{5.82}Al_{0.18})O_{27}O_{0.35}(OH_{3.65})$
8.	$(Na_{1.04}Ca_{0.10}K_{0.10})(Al_{1.95}Li_{0.59}\square_{0.22}Fe^{2+}_{0.18}Mn_{0.04}Mg_{0.02})Al_6B_{2.96}(Si_{5.86}Al_{0.14})O_{27}O_{1.02}(OH_{2.93}F_{0.05})$

1. Swanson et al. (1964)
2. Simpson (1931)
3. Takeshi (1953)
4. Chebotarev et al. (1971)
5. El-Hinnawi et al. (1966)
6. El-Hinnawi et al. (1966)
7. Chaudhry and Howie (1976)
8. Sjögren (1916)

following observations regarding the extent of solid solution in natural tourmalines between the end-members: schorl–dravite, $Na(Fe,Mg)_3Al_6(BO_3)_3Si_6O_{18}(OH)_4$; elbaite, $Na(Li,Al)_3Al_6(BO_3)_3Si_6O_{18}(OH)_4$; and $R^+R_3^{3+}R_6^{3+}(BO_3)_3Si_6O_{18}O_3(OH)$, where R^+ and R^{3+} are principally Na^+ and Al^{3+}, respectively (see Fig. 9 in Foit and Rosenberg, 1977).

(1) While a few samples approximating end-member schorl/dravite have been observed, elbaites closely approaching end-member composition have not been reported; all are appreciably Li-deficient and Al-rich. Although liddicoatite, the Ca-analog of elbaite (Dunn *et al.*, 1977) has a Li/Al ratio higher than that of elbaite, it is also Li-deficient with respect to its idealized end-member composition.

(2) Most tourmalines which approach to within 90 mole percent of end-member schorl/dravite are Mg-rich.

(3) Substitution of R^{3+} for Mg^{2+}, Fe^{2+} or Li^+ in the 9b site is extremely common and generally more extensive in the elbaites than in the schorls and dravites.

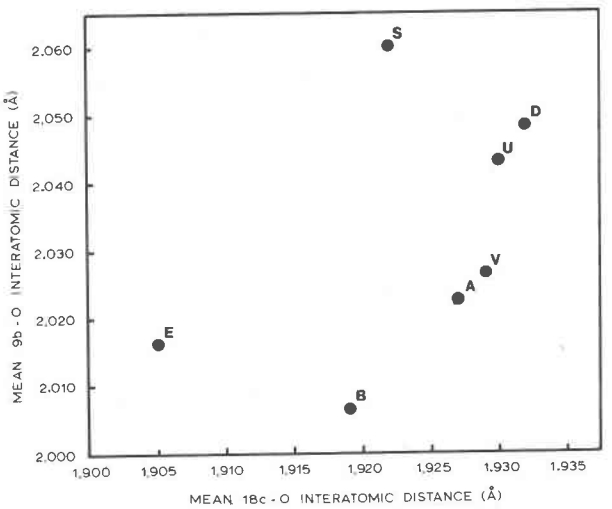

Fig. 8. Variation of mean 9b–O interatomic distance with mean 18c–O interatomic distance.

(4) Li substitution in schorls and dravites is far more limited than Fe and Mg substitution in elbaites.

The preferential incorporation of higher field

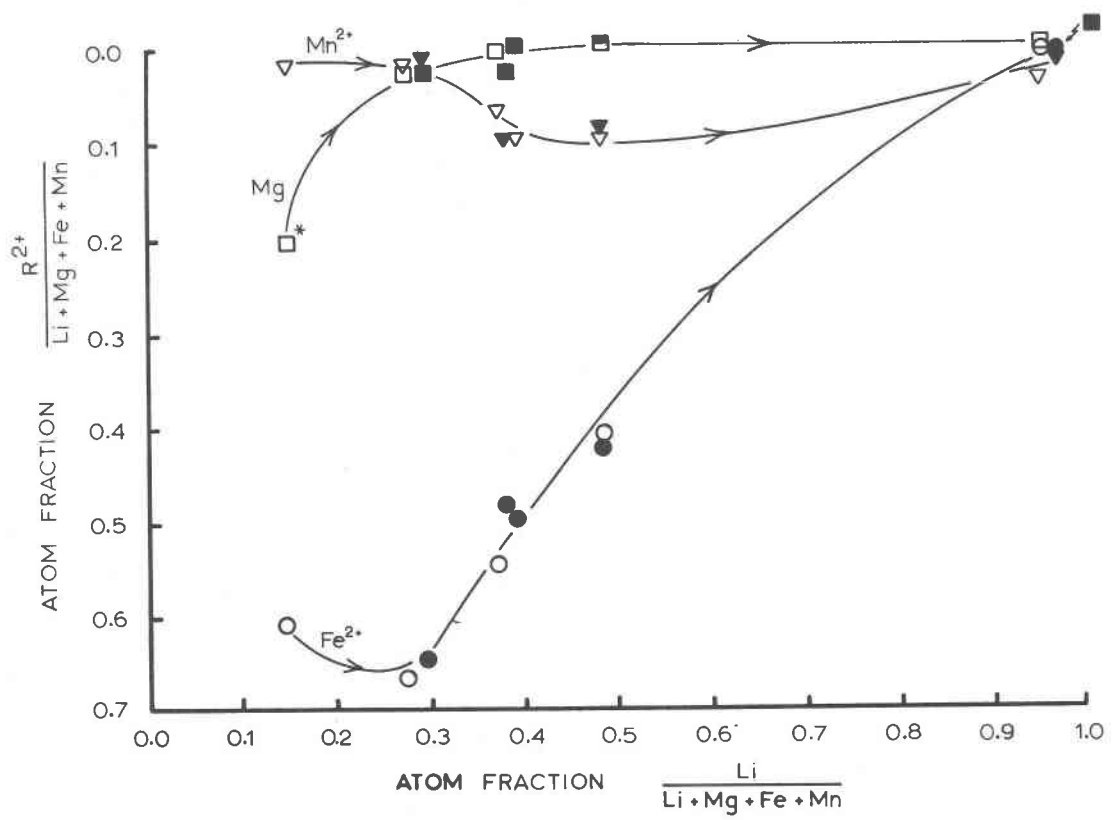

Fig. 9. Variations in the Mg–, Fe^{2+}–, Mn^{2+}–, and Li-content of tourmalines from the Brown Derby pegmatites; calculated from the data of Staatz *et al.* (1955). Squares, Mg/(Li + Mg + Fe + Mn); circles, Fe^{2+}/(Li + Mg + Fe + Mn); triangles, Mn^{2+}/(Li + Mg + Fe + Mn). Open symbols, Brown Derby No. 2 pegmatite, filled symobols, Brown Derby No. 3 pegmatite. Arrows show direction of change during crystallization from the walls inward toward the core. (*), Mg value used is a minimum.

strength cations (Al^{3+}, Fe^{3+}) implied by these relationships is facilitated by the apparent ease of proton exchange which serves to maintain charge balance.

Although diverse substitutions in the tourmaline structure do result in significant systematic changes in polyhedral distortion (Figs. 1–4), distortion itself does not appear to play a major role in limiting substitution. The nature and extent of cation substitution in tourmaline appears to be more closely governed by fractionation resulting from differences in cation field strength. Substitution of high field strength cations generally results in improved local charge balance (Foit and Rosenberg, 1977) which undoubtedly facilitates these substitutions.

Acknowledgments

The authors are indebted to Dr. Kenneth G. Snetsinger, Space Sciences Division, NASA Ames Research Center, for information regarding the location of the V-tourmaline deposit; Mr. David Plant, Department of Geology, Manchester University, for the electron microprobe analysis, Professor Roger D. Willett, Department of Chemistry, Washington State University, for the use of his automated single-crystal diffractometer, and Ms. Julie V. Jaquish for collection and reduction of the X-ray data. We also thank Professor Wayne A. Dollase, Department of Earth and Space Sciences, University of California, Los Angeles, and Professor Gabrielle Donnay, Department of Geological Sciences, McGill University, for critically reviewing the manuscript.

References

Barton, Jr., R. (1969) Refinement of the crystal structure of buergerite and the absolute orientation of tourmalines. *Acta Crystallogr., B25,* 1524–1533.

Buerger, M. J., C. W. Burnham and D. R. Peacor (1962) Assessment of several structures proposed for tourmaline. *Acta Crystallogr., 15,* 583–590.

Busing, W. R., K. O. Martin and H. A. Levy (1962) A Fortran crystallographic least squares program. *U.S. Nat. Tech. Inform. Serv.,* ORNL-TM-305.

———, ——— and ——— (1964) A Fortran crystallographic function and error program. *U.S. Nat. Tech. Inform. Serv.,* ORNL-TM-306.

Chaudhry, M. N. and R. A. Howie (1976) Lithium tourmalines from the Meldon aplite, Devonshire, England. *Mineral. Mag., 40,* 747–751.

Chebotarev, G. M. and G. P. Chebotareva (1971) Dravite variety of tourmaline from Muruntau (western Uzbekistan). *Zap. Uzbekistansk. Otd. Vses. Mineral. Obshchest., 24,* 112–115.

Cromer, D. T. and J. T. Waber (1965) Scattering factors computed from relativistic Dirac–Slater wave functions. *Acta Crystallogr., 18,* 104–109.

Donnay, G. and R. Allmann (1970) How to recognize O^{2-}, $(OH)^-$ and H_2O in crystal structures determined by X-rays. *Am. Mineral., 55,* 1003–1015.

——— and R. Barton, Jr. (1972) Refinement of the crystal structure of elbaite and the mechanism of tourmaline solid solution. *Tschermaks Mineral. Petrog. Mitt., 18,* 273–286.

Dunn, P. J., D. E. Appleman and J. E. Nelen (1977) Liddicoatite, a new calcium end-member of the tourmaline group. *Am. Mineral., 62,* 1121–1124.

El-Hinnawi, E. E. and R. Hofmann (1966) Optical and chemical investigation of nine tourmalines (elbaite). *Neues Jahrb. Mineral. Monatsh,* 80–88.

Epprecht, W. (1953) Die Gitterkonstanten der Turmalin. *Schweiz. Mineral. Petrog. Mitt., 33,* 481–505.

Foit, Jr., F. F. and P. E. Rosenberg (1974) Coupled substitutions in tourmaline (abstr.). *EOS, Trans. Am. Geophys. Union, 55,* 467.

——— and ——— (1975) Aluminobuergerite, $Na_{1+x}R^{3+}_3R^{3+}_6(BO_3)_3Si_6O_{18}O_{3-x}(OH)_{1+x}$, a new end-member of the tourmaline group (abstr.). *EOS, Trans. Am. Geophys. Union, 56,* 461.

——— and ——— (1977) Coupled substitutions in the tourmaline group. *Contrib. Mineral. Petrol., 62,* 109–127.

Fortier, S. and G. Donnay (1975) Schorl refinement showing compositional dependence of the tourmaline structure. *Can. Mineral., 13,* 173–177.

Robinson, K., G. V. Gibbs and P. H. Ribbe (1971) Quadratic elongation: a quantitative measure of distortion in coordination polyhedra. *Science, 172,* 567–570.

Rosenberg, P. E. and F. F. Foit, Jr. (1975) Alkali-free tourmalines in the system MgO–Al_2O_3–SiO_2–H_2O–B_2O_3 (abstr.). *Geol. Soc. Am. Abstracts with Programs, 7,* 1250.

——— and ——— (1977) Crystal chemistry of alkali-free tourmaline (abstr.). *Geol. Soc. Am. Abstracts with Programs, 9,* 1147–1148.

Schemtzer, K. (1978) *Vanadium III als Farbträger bei naturlichen Silicaten und Oxiden-ein Beitrag zur Kristallchemie des Vanadiums.* Doctoral Dissertation, Ruprecht-Karl-Universität, Heidelberg.

Shannon, R. D. (1976) Revised effective ionic radii and systematic studies of interatomic distances in halides and chalcogenides. *Acta Crystallogr., A32,* 751–767.

Simpson, E. S. (1931) Contributions to the mineralogy of Western Australia. IV. *J. Roy. Soc. W. Australia, 17,* 137–149.

Sjögren, H. (1916) The chemical composition of tourmaline from Utö. *Bull. Geol. Inst. Univ. Upsala, 15,* 317–324.

Snetsinger, K. G. (1966) Barium–vanadium muscovite and vanadium tourmaline from Mariposa County, California. *Am. Mineral., 51,* 1623–1639.

Staatz, M. H., K. J. Murata and J. J. Glass (1955) Variation of composition and physical properties of tourmaline with its position in the pegmatite. *Am. Mineral., 40,* 789–804.

Swanson, H. E., M. C. Morris, E. H. Evans and L. Verner (1964) Standard X-ray diffraction patterns. *U.S. Nat. Bureau of Standards, Mem. 25, Part 1; Sec. 3,* 47–48.

Takeshi, H. (1953) White tourmaline from Kanakura Mine, Nagano Prefecture, Japan. *J. Mineral. (Japan), 1,* 105–112.

Tippe, A. and W. C. Hamilton (1971) A neutron-diffraction study of the ferric tourmaline, buergerite. *Am. Mineral., 56,* 101–113.

Tsang, T., A. N. Thorpe and G. Donnay (1971) Magnetic susceptibility and triangular exchange coupling in the tourmaline mineral group. *J. Phys. Chem. Solids, 32,* 1441–1448.

Walsh, D., G. Donnay and J. D. H. Donnay (1974) Jahn-Teller effects in ferromagnesian minerals: pyroxenes and olivines. *Bull. Soc. fr. Mineral. Crystallogr., 97,* 170–183.

Weyl, W. A. and E. C. Marboe (1962) *The Constitution of Glasses: a Dynamic Interpretation.* Interscience-Wiley, New York.

Manuscript received, September 26, 1978;
accepted for publication, February 28, 1979.